

# Properties of surface layers formed on lithium in Li-SOCl<sub>2</sub> cells: synergetic effect of SO<sub>2</sub> and LiAl(SO<sub>3</sub>Cl)<sub>4</sub>

P. CHENEBAULT, D. VALLIN

*S.A.F.T. Département des générateurs de technologies avancées, rue Georges Leclanché, B.P. 357, 86009 Poitiers, France*

J. THEVENIN, R. WIART

*Physique des Liquides et Electrochimie, Laboratoire Propre du C.N.R.S., associé à l'Université Paris VI, place Jussieu, 75230 Paris cedex 05, France*

Received 4 November 1987; revised 11 February 1988

Kinetic and morphological properties of surface layers formed on the Li anode during storage in SOCl<sub>2</sub>/LiAlCl<sub>4</sub> solution have been investigated. The synergetic effect of SO<sub>2</sub> and LiAl(SO<sub>3</sub>Cl)<sub>4</sub>, used for voltage delay alleviation, changes the shape and size of the microcrystals of LiCl constituting the surface layer. It also leads to separate and modify the conduction and charge transfer processes involved in the kinetic properties of the surface layer at the equilibrium potential. These properties appear to be similar to those of a polycrystalline solid electrolyte where the grain boundaries induce an intergranular conduction process.

## 1. Introduction

In the field of primary cells, the Li/LiAlCl<sub>4</sub>-SOCl<sub>2</sub>/C system has been extensively investigated over the last decade. This system has received particular attention because of its relatively high open-circuit voltage and high energy density [1]. The cell discharge is however affected by the properties of the LiCl surface layer formed on the Li electrode during storage [2]. The voltage delay effect, which results in a voltage drop followed by a slow recovery during the discharge, can reduce the field of application of such liquid cathode primary batteries.

Morphological and kinetic studies of the lithium chloride surface layer have not yet completely revealed the elementary processes resulting in the voltage delay effect [2-4]. Numerous studies have been devoted to the variables which might affect the layer properties. These variables include composition and concentration of the electrolyte, and presence of organic and inorganic additives [5-13]. As far as inorganic additives are concerned, few have been proven to be sufficient for many storage and test conditions [8, 9]. Recently, it has been shown that a new inorganic compound LiAl(SO<sub>3</sub>Cl)<sub>4</sub>, used with SO<sub>2</sub>, allows alleviation of the voltage delay effect [10].

The aim of this paper is to study the kinetic and morphological properties of the surface layers formed in a thionyl chloride solution using these inorganic additives.

## 2. Experimental details

### 2.1. Solutions

The solution of LiAlCl<sub>4</sub> in SOCl<sub>2</sub> was prepared by dissolving the required amount of AlCl<sub>3</sub> in SOCl<sub>2</sub>, followed by the addition of a slight excess of LiCl. Solution with SO<sub>2</sub> was prepared by total neutralization of AlCl<sub>3</sub>/SOCl<sub>2</sub> by Li<sub>2</sub>CO<sub>3</sub>.

Solution with LiAl(SO<sub>3</sub>Cl)<sub>4</sub> (lithium tetrachloro sulfato aluminate) was prepared according to a procedure previously described [10, 14, 18], in which small amounts of HSO<sub>2</sub>Cl are added to the electrolyte. The *in situ* reaction with LiAlCl<sub>4</sub> leads to the formation of LiAl(SO<sub>3</sub>Cl)<sub>4</sub> and HCl is eliminated by refluxing the electrolyte. Another procedure [15, 16] led to the preparation of LiAl(SO<sub>3</sub>Cl)<sub>4</sub> in liquid SO<sub>2</sub> by reacting SO<sub>3</sub> and LiAlCl<sub>4</sub>. The compound was easily isolated and the required amount was then directly added to the electrolyte.

For the present study, four solutions have been termed:

the 'reference solution': SOCl<sub>2</sub> + 1.35 M LiAlCl<sub>4</sub>

the 'solution with SO<sub>2</sub>':

SOCl<sub>2</sub> + 1.35 M LiAlCl<sub>4</sub> + 0.5 M SO<sub>2</sub>

the 'solution with LiAl(SO<sub>3</sub>Cl)<sub>4</sub>':

SOCl<sub>2</sub> + 1.35 M LiAlCl<sub>4</sub> + 0.017 M LiAl(SO<sub>3</sub>Cl)<sub>4</sub>

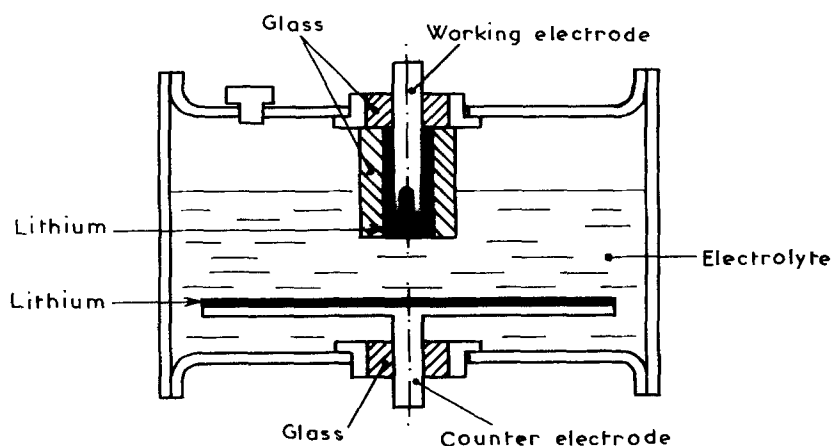


Fig. 1. Schematic view of the two-electrode cell used for impedance measurements.

the 'complete solution':  $\text{SOCl}_2 + 1.35 \text{ M LiAlCl}_4$   
 $+ 0.5 \text{ M SO}_2 + 0.017 \text{ M LiAl(SO}_3\text{Cl)}_4$

The optimal concentrations of both additives have been defined according to a previous study of their effect on the voltage delay alleviation [10, 18].

## 2.2. Electrochemical cell

For this investigation, a specially designed two-electrode cell [18] has been used, as shown in Fig. 1. The electrodes were disks of lithium (Foote Mineral, purity 99.9%). The surface area of the working electrode ( $0.07 \text{ cm}^2$ ) was much smaller than that of the counter electrode ( $28 \text{ cm}^2$ ). The hermetic and cylindrical cell container was made of stainless steel. The lithium electrode, fitted in a glass tube, was connected to the top of the cell container by using the central pin of a glass/metal seal. The volume of the liquid solution was about  $8.5 \text{ cm}^3$  representing 75% of the internal volume of the cell container.

## 2.3. Morphological studies

After storage the lithium electrodes were washed in pure  $\text{SOCl}_2$  solvent. The surface layer was observed by means of scanning electron microscopy. A transfer device described elsewhere [17] prevents the atmospheric contamination of the electrode during its transportation from the glove box. The thickness of the surface layer was determined by observation of a longitudinal cross section of the electrode. The microscope was also fitted with an X-ray analyser able to detect elements of relatively high atomic number present in the surface layer.

## 2.4. Kinetic studies

Impedance measurements were performed using a frequency-response analyser (Solartron 1174) monitored by a microcomputer (Apple II). A galvanostat was used to superimpose a sinusoidal signal of a few  $\mu\text{A cm}^{-2}$  at the equilibrium potential of the lithium electrode. Such an amplitude of the a.c. signal was sufficiently low to maintain linear conditions and to avoid any change in the steady state potential.

According to the ratio between the surface areas of the electrodes, the measured impedance results mainly from the working electrode behaviour. The impedance diagrams, over a wide frequency range ( $5 \times 10^5$  to  $5 \times 10^{-3} \text{ Hz}$ ), were automatically plotted in the complex plane on a printer connected to the microcomputer.

## 3. Results and discussion

### 3.1. Morphological properties of the surface layer

The LiCl polycrystalline layer was clearly identified by X-ray analysis whatever the storage time. The presence of the elements Al and S on the surface layer can be attributed to traces of the solute and solvent

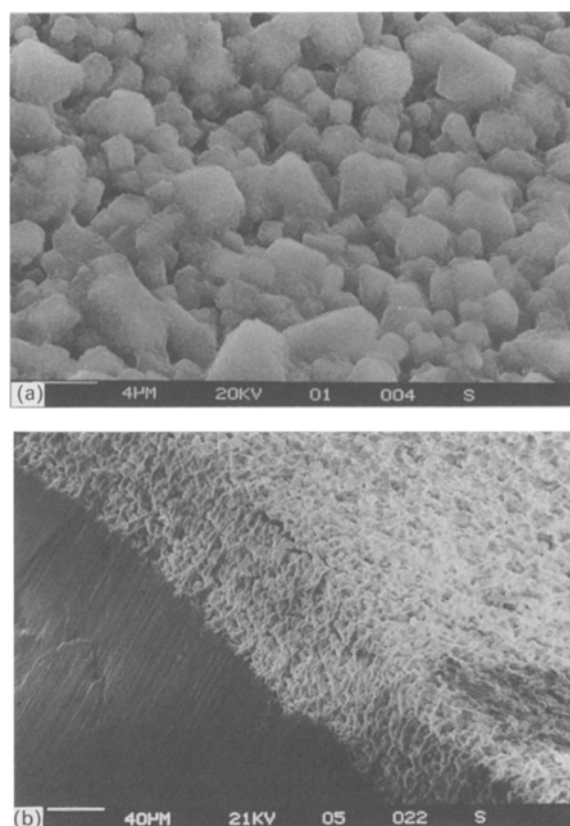


Fig. 2. Morphology of the surface layer formed on the lithium electrode after 1 month storage in the 'reference solution'. (a) Structural aspect, (b) longitudinal cross section.

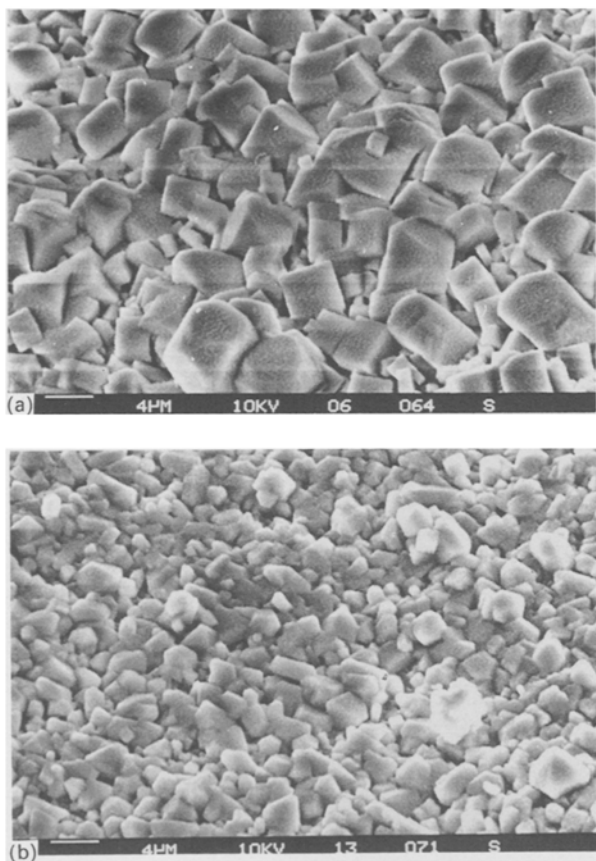


Fig. 3. Structural aspect of the surface layer formed on the lithium electrode after 1 month storage in different test solutions. (a) 'Solution with SO<sub>2</sub>', (b) 'solution with LiAl(SO<sub>3</sub>Cl)<sub>4</sub>'.

from the solutions studied independently of the presence of the inorganic additives.

After 1 month storage, the synergetic effect of the additions on the morphological properties of the surface layer can be easily demonstrated. For the 'reference solution', as shown in Fig. 2a, the surface layer consisted of a great number of microcrystals (average size of 2 μm), and without any well-defined geometry. The layer thickness was of the order of 80 μm, as shown in Fig. 2b. For the 'solution with SO<sub>2</sub>', as shown in Fig. 3a, the microcrystals have approximately the same size as those observed in the 'reference solution', but they have a more evident cubic geometry. For the 'solution with LiAl(SO<sub>3</sub>Cl)<sub>4</sub>', as shown in Fig. 3b, the microcrystals keep their cubic geometry, but are smaller and more numerous (average size of 1 μm) than those observed in the 'reference solution'. For the 'complete solution', as shown in Fig. 4a, the surface layer consisted of large cubic crystals (with a size up to 60 μm) exhibiting the (100) and (111) planes, and coexisting with numerous smaller crystals. The maximum thickness was about 40 μm, while the minimum thickness was about 10 μm, as shown in Fig. 4b.

Accordingly, the synergetic effect of the additives SO<sub>2</sub> and LiAl(SO<sub>3</sub>Cl)<sub>4</sub> in the 'complete solution' modifies both the size and shape of the LiCl microcrystals, and leads to the formation of a surface layer more heterogeneous than in the 'reference solution' [18]. As demonstrated for other alkaline halogenides

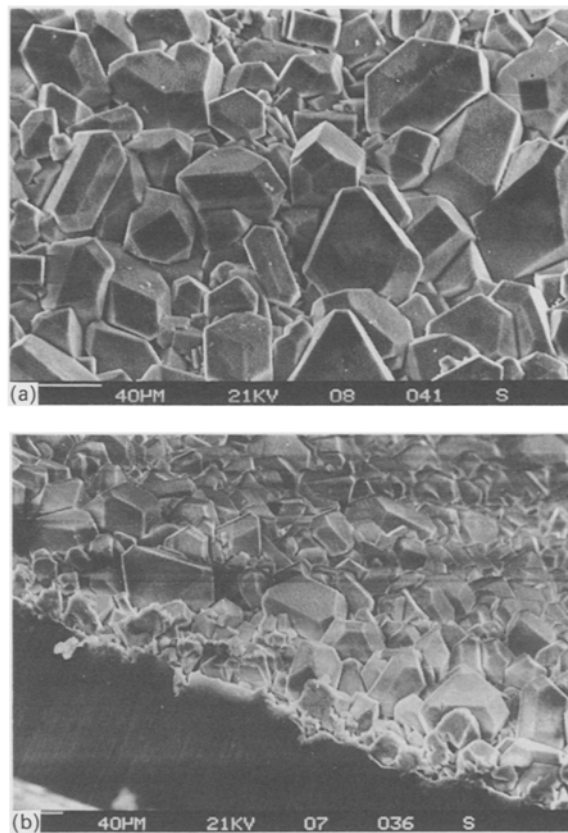


Fig. 4. Morphology of the surface layer formed on the lithium electrode after 1 month storage in the 'complete solution'. (a) Structural aspect, (b) longitudinal cross section.

[19], the formation of particular planes can probably be related to a specific adsorption of the additives on the surface layer. There is no evidence of a thin compact primary sublayer covered with a thick porous secondary sublayer, in spite of the common assumption concerning the stratified structure of the surface layer [20].

### 3.2. Kinetic properties of the surface layer

**3.2.1. Interphase model.** The LiCl surface layer acts as a solid electrolyte interphase between the lithium electrode and the aprotic electrolyte. Extensive studies have demonstrated the influence of the polycrystalline structure of the solid electrolyte on its kinetic properties between two non-blocking electrodes [21, 22].

Typical polycrystalline solid electrolytes, such as sinters or compacted powders, can be schematically represented, as shown in Fig. 5a. The crystals (grains) are in contact with the others on limited surface areas (grain boundaries), so that voids are possible in the structure of the solid electrolyte. Accordingly, the average conductivity of such a system has two components: the intragranular conductivity  $\sigma_a$  of each crystal, and the intergranular conductivity  $\sigma_c$  between two adjacent crystals. As shown in Figs 5b and 5c, the equivalent circuit and the impedance diagram in the complex plane are represented as follows:

— the first circuit, due to the intragranular conduction process, is represented by a bulk resistance,  $R_b$ ,

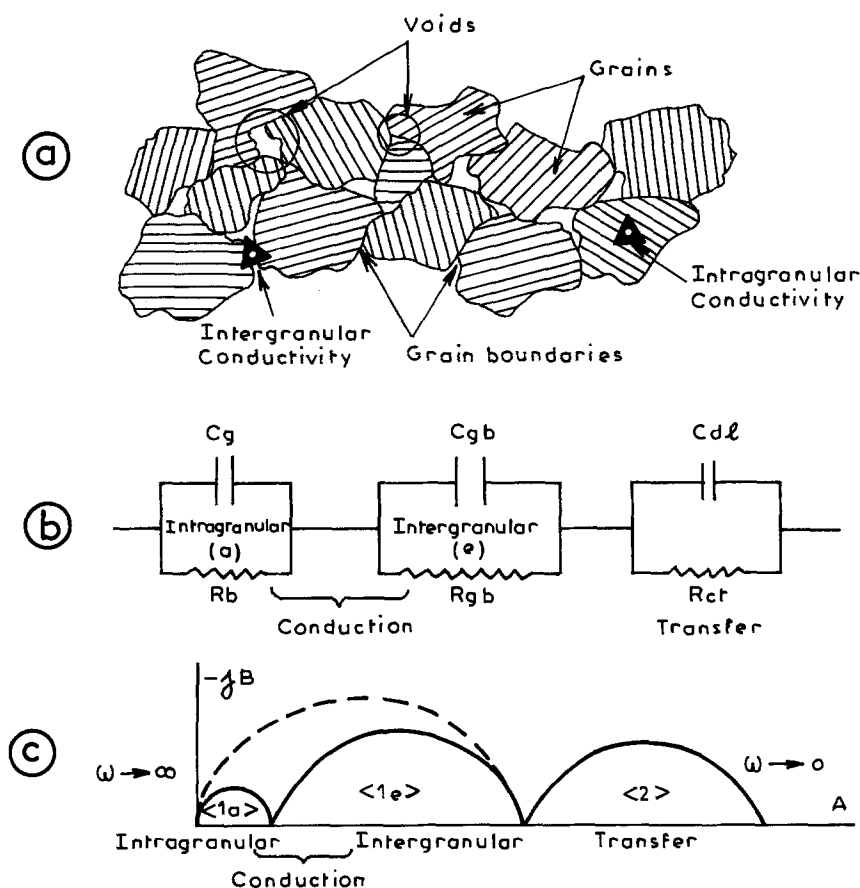


Fig. 5. Polycrystalline interphase model. (a) Schematic presentation of the surface layer, (b) equivalent electrical circuit, (c) impedance diagram in the complex plane.

and a geometric capacitance,  $C_g$ . Considering the solid electrolyte as a single crystal, these components are associated with the intragranular parameters, such as conductivity,  $\sigma_a$ , and permittivity,  $\epsilon_a$ , by the classical equations:

$$R_b = d/\sigma_a A \quad \text{and} \quad C_g = \epsilon_a A/d$$

where  $A$  is the electrode surface area, and  $d$  the thickness of the solid electrolyte. The capacitive semicircle  $\langle 1a \rangle$ , associated to this intragranular conduction process, is observed in the high frequency range.

— the second circuit, due to the intergranular conduction process, is related to the properties of the grain boundaries in the polycrystalline solid electrolyte. It is represented by a grain boundary resistance,  $R_{gb}$ , and a grain boundary capacitance,  $C_{gb}$ . Similarly to the preceding circuit, these components can be associated to the intergranular parameters  $\sigma_e$  and  $\epsilon_e$ , which are different from the intragranular parameters  $\sigma_a$  and  $\epsilon_a$ . The capacitive semicircle  $\langle 1e \rangle$  associated to this intergranular conduction process is generally observed in the medium frequency range.

— the third circuit is related to the charge transfer process occurring at the metal/layer interface. It is represented by a charge transfer resistance,  $R_{ct}$ , and a double layer capacitance,  $C_{dl}$ . The capacitive semicircle  $\langle 2 \rangle$  associated with the charge transfer process is observed in the medium and low frequency ranges.

From a practical point of view, by considering the limited high frequencies which can be used for electrode

impedance spectroscopy, it appears that, essentially, the intergranular conduction and charge transfer processes can be conveniently studied by analysis of the capacitive semicircles  $\langle 1e \rangle$  and  $\langle 2 \rangle$ . In addition, when the time constants of the elementary processes are of the same order, these processes cannot be easily separated on the impedance diagram, as illustrated in Fig. 5c (dashed line) for the intragranular and intergranular conduction processes. Moreover, the fact that the centre of each semicircle is currently lying under the real axis in the complex plane reveals a frequency dispersion of the resistance and/or capacitance associated with the process [23]. This dispersion is generally attributed to a statistical distribution of the resistive and dielectric properties inside the polycrystalline solid electrolyte.

**3.2.2. Results.** The kinetic properties of the surface layers as a function of the storage time in the different solutions can be analysed within the framework of the preceding interphase model, particularly in order to point out the synergetic effect of the additives  $\text{SO}_2$  and  $\text{LiAl}(\text{SO}_3\text{Cl})_4$  at any time during the storage of the Li electrode in the  $\text{SOCl}_2/\text{LiAlCl}_4$  solution.

During the first day of storage, as shown in Fig. 6, two capacitive semicircles  $\langle 1 \rangle$  and  $\langle 2 \rangle$  in the high and low frequency ranges are observed whatever the solutions. In a first approach, regarding the time constants of the two processes considered, the semicircle  $\langle 1 \rangle$  can be essentially ascribed to the intergranular

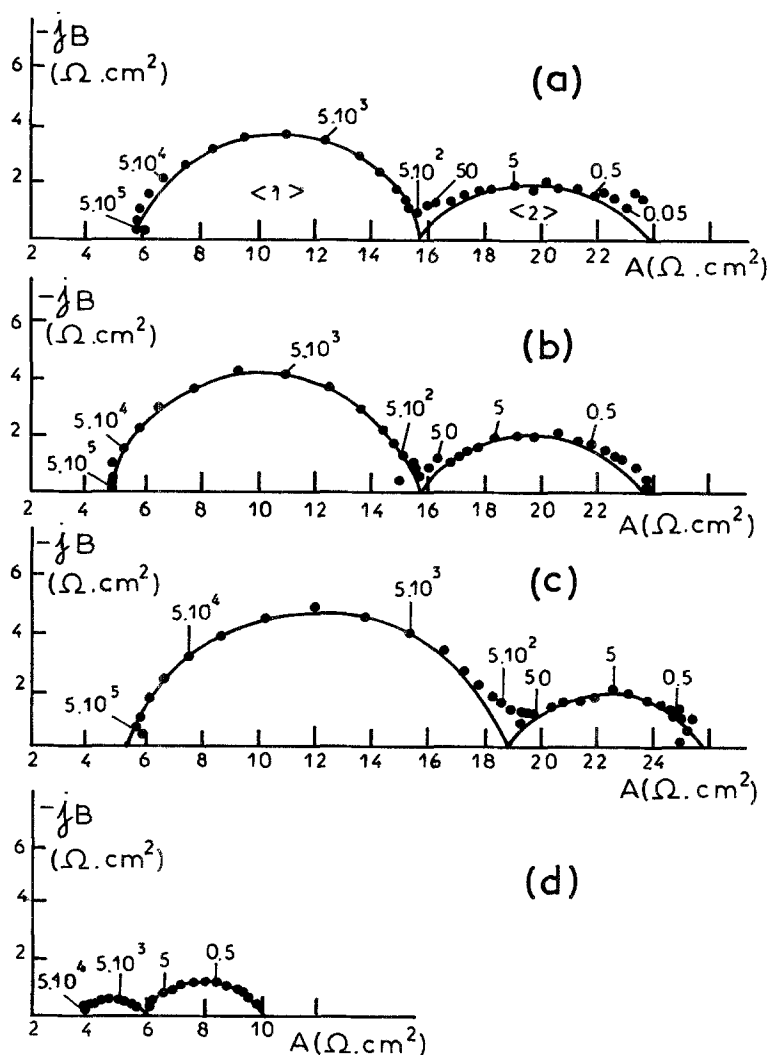


Fig. 6. Impedance behaviour of the surface layer formed on the lithium electrode after 1 day storage in different solutions: (a) 'reference solution', (b) 'solution with SO<sub>2</sub>', (c) 'solution with LiAl(SO<sub>3</sub>Cl)<sub>4</sub>', (d) 'complete solution'. The impedance diagrams in the complex plane are given with frequencies in Hz.

conduction process, while the semicircle <2> can be related to the charge transfer process. The same ratio  $R_{gb}/R_{ct}$  larger than unity and the same polarization resistance ( $R_{gb} + R_{ct}$ ) of about 20 ohm cm<sup>2</sup> were calculated for the 'reference solution' (Fig. 6a), the 'solution with SO<sub>2</sub>' (Fig. 6b) and the 'solution with LiAl(SO<sub>3</sub>Cl)<sub>4</sub>' (Fig. 6c). On the contrary, a ratio  $R_{gb}/R_{ct}$  lower than unity and a smaller polarization resistance ( $R_{gb} + R_{ct}$ ) of 6 ohm cm<sup>2</sup> were determined for the 'complete solution'.

The variation of the impedance diagrams depends on the solution used during the storage of the lithium electrode at ambient temperature, as shown in Figs 7 and 8. For the 'reference solution' and the 'solution with SO<sub>2</sub>', as shown in Figs 7a and 7b, respectively, the semicircle <2> progressively disappeared, while the semicircle <1> continuously increased with the storage time. For the 'solution with LiAl(SO<sub>3</sub>Cl)<sub>4</sub>', as shown in Fig. 8a, the remaining semicircle <1> increased with a half size at any storage time by comparison to Fig. 7a. For the 'complete solution', as shown in Fig. 8b, the semicircles <1> and <2> remained well defined over the whole frequency range, the resistances  $R_{gb}$  and  $R_{ct}$  appearing to increase in the same manner during storage, and the polarization resistance ( $R_{gb} + R_{ct}$ ) remained two times lower than that determined for the 'reference solution'. After 1 month of storage, for the 'reference and complete solutions',

the values of the resistance  $R_{gb}$  were 800 ohm cm<sup>2</sup> and 200 ohm cm<sup>2</sup>, respectively, while those of the capacitance  $C_{gb}$  were 0.5 μF cm<sup>-2</sup> and 0.1 μF cm<sup>-2</sup>, respectively. Then for the 'complete solution', the value of the resistance  $R_{ct}$  was 250 ohm cm<sup>2</sup> and the capacitance  $C_{ct}$  was 100 μF cm<sup>-2</sup>.

Consequently, the synergetic effect of the inorganic additives SO<sub>2</sub> and LiAl(SO<sub>3</sub>Cl)<sub>4</sub> has been verified by the analysis of the relative importance of the two elementary processes on the impedance diagrams [18]. The kinetic properties of the surface layer formed in the 'complete solution' appear to be modified in a proper way so that the intergranular conduction resistance,  $R_{gb}$ , is reduced while the charge transfer resistance,  $R_{ct}$ , is increased. The additives, leading to a decrease of the thickness and resistance of the surface layer, are also able to enhance the inhibition of the charge transfer at the metal/layer interface. The fact that the polarization resistance was considerably lower for the 'complete solution' when compared to the 'reference solution' is certainly one reason for the alleviation of the voltage delay in the presence of the inorganic additives. Another reason for the voltage delay alleviation probably lies in the variation of the charge transfer resistance with storage time.

3.2.3. Discussion. A previous model for the study of

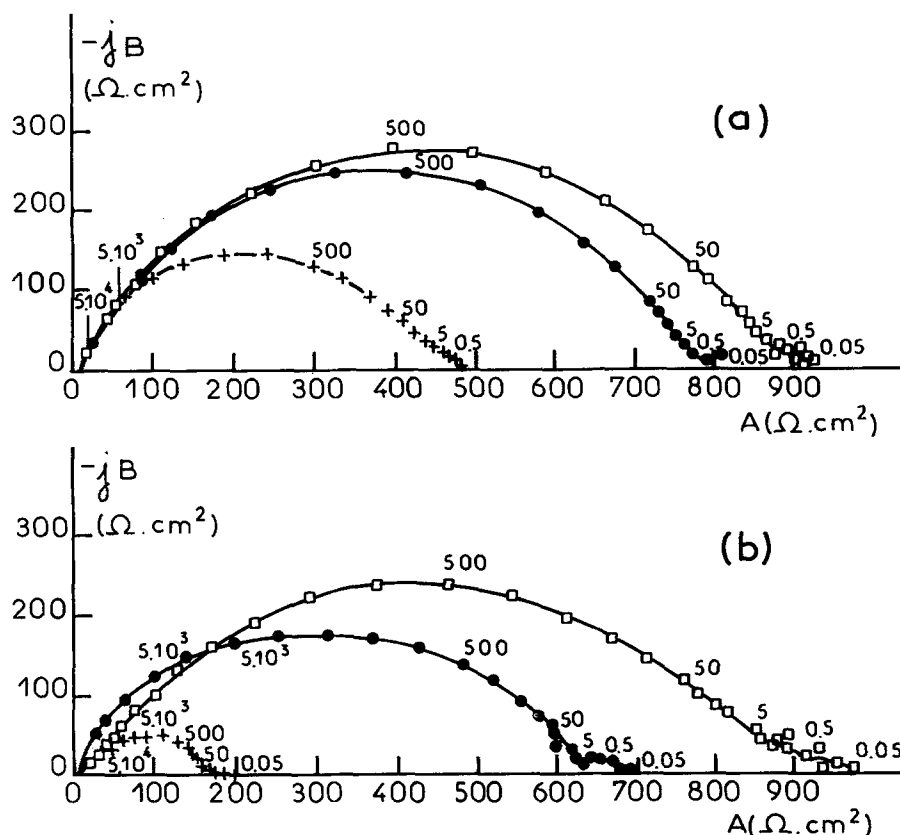


Fig. 7. Influence of the storage time up to 1 month on the impedance behaviour of the surface layer formed on the lithium electrode in different solutions: (a) 'reference solution', (b) 'solution with  $\text{SO}_2$ '. The impedance diagrams are given with frequencies in Hz. (+) After 2 days, (●) after 2 weeks, (□) after 1 month.

the surface layer, the 'solid electrolyte interphase' model, has been described [3, 20] in order to directly evaluate the thickness of the surface layer from its kinetic properties. By assuming a relative permittivity given in the literature (of the order of 10 for LiCl), the

determination of the conduction capacitance generally leads to the evaluation of an apparent thickness several orders lower than the total thickness of the surface layer effectively observed on the lithium electrode. In order to explain such unexpected results, it

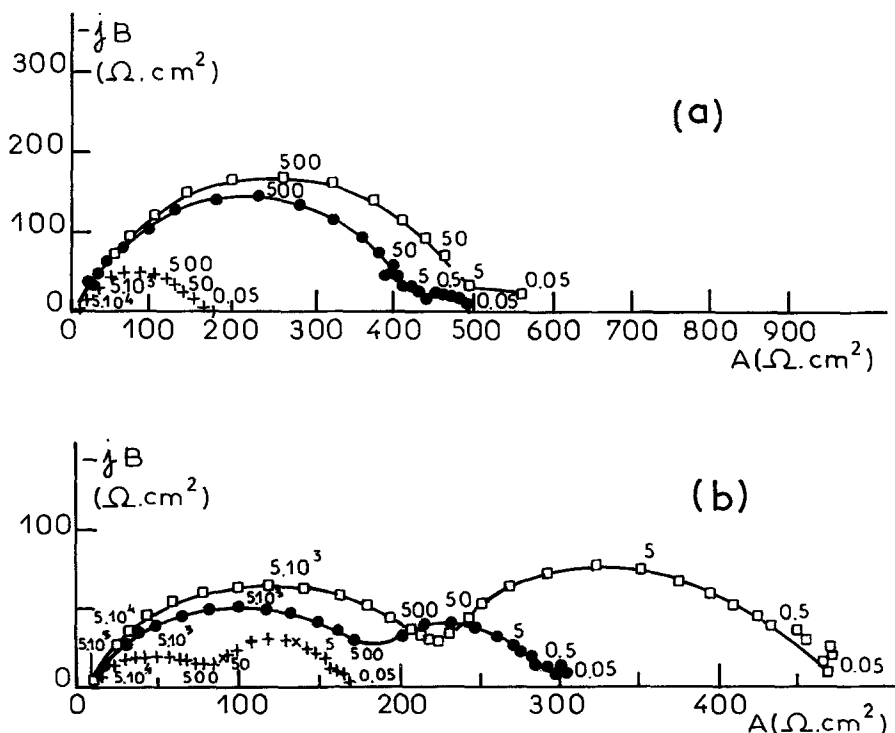


Fig. 8. Influence of the storage time up to 1 month on the impedance behaviour of the surface layer formed on the lithium electrode in different solutions: (a) 'solution with  $\text{LiAl}(\text{SO}_3\text{Cl})_2$ ', (b) 'complete solution'. The impedance diagrams are given with frequencies in Hz. (+) After 2 days, (●) after 2 weeks, (□) after 1 month.

has been assumed that the surface layer was stratified and constituted, at least, by two sublayers, a thin compact primary sublayer and a thick porous secondary sublayer [20, 24–27]. The whole kinetic properties of the surface layer at the equilibrium potential are attributed to the compact primary sublayer, the thickness of which was determined by kinetic methods. It is also assumed that the porous secondary sublayer, the thickness of which was evaluated by the difference between the thicknesses measured by optical and kinetic methods, was at the origin of the voltage delay effect occurring during the anodic polarization. In addition to the fact that a stratified interphase model does not make clear the elementary processes involved in the surface layer, it is necessary to note that the main assumptions of such a model have not been verified by experiments. Moreover, it is rather difficult to conceive that more than 99% of the total thickness of the surface layer was without any effect on the properties of the metal/layer interface at the equilibrium potential.

The proposed polycrystalline interphase model is an attractive alternative to reconcile the morphological and kinetic data by pointing out that the intergranular permittivity,  $\epsilon_c$ , is specific of the structure of the solid electrolyte and not directly related to the intragranular permittivity,  $\epsilon_a$ , of the single crystal of the same solid electrolyte. Consequently, the thickness of the polycrystalline surface layer cannot be deduced from the equation of the capacitance by using any value of the permittivity taken in the literature. Accordingly, the stratified interphase model appears to be based on a misunderstanding of the importance of the intragranular and intergranular conduction processes in the polycrystalline solid electrolyte. In spite of its limited field of application, the polycrystalline interphase model gives the opportunity to determine the intergranular conductivity,  $\sigma_c$ , as a function of the presence of the additives in the solution. For the 'reference solution', a total thickness,  $d$ , of 80  $\mu\text{m}$  for a grain boundary resistance  $R_{\text{gb}}$  of 800  $\text{ohm cm}^2$  leads to a value of  $\sigma_c$  of the order of  $10^{-5} \text{ S cm}^{-1}$ . The same value is obtained for the 'complete solution' (average thickness of 20  $\mu\text{m}$  and grain boundary resistance of 200  $\text{ohm cm}^2$ ) although the surface layer was constituted by a number of larger crystals. This relatively high value of the intergranular conductivity, which lies between the average conductivity of the solid electrolyte ( $10^{-10} \text{ S cm}^{-1}$ ) and that of the liquid solution ( $10^{-2} \text{ S cm}^{-1}$ ), leads one to consider at least two hypotheses to understand an enhanced conduction process in the surface layer. One hypothesis is to suppose that the layer conductivity is increased by the inclusion at the grain boundaries of conductive compounds such as the solute  $\text{LiAlCl}_4$  (conductivity of  $10^{-4} \text{ S cm}^{-1}$ ). Another hypothesis is to suppose that the surface layer is microporous, the voids, or pores, being filled by the liquid solution.

#### 4. Conclusion

This study has demonstrated the synergetic effect of

the inorganic additives  $\text{SO}_2$  and  $\text{LiAl}(\text{SO}_3\text{Cl})_4$  on the morphological and kinetic properties of  $\text{LiCl}$  surface layers formed in the  $\text{SOCl}_2/\text{LiAlCl}_4$  solution, where such additives are used for alleviation of the voltage delay effect.

Modifications of the shape and size of the  $\text{LiCl}$  microcrystals due to the presence of additives in the solution have been observed by scanning electron microscopy. Variations of the elementary processes involved in the surface layer, such as the intergranular conduction and charge transfer processes, have been analysed by electrode impedance spectroscopy. During storage time, it has been shown that the impedances corresponding to these processes can be well separated with similar significance in the electrode polarization.

The properties of the polycrystalline  $\text{LiCl}$  surface layer considered as a solid electrolyte interphase can be assumed to be similar to those of sinters or compacted powders, where the grain boundaries determine an intergranular conductivity. This conductivity, close to  $10^{-5} \text{ S cm}^{-1}$ , is not affected by the additives which reduce the layer thickness.

The proposed polycrystalline interphase model shows that the layer thickness cannot be deduced from kinetic measurements in the absence of any information concerning the effective values of the intergranular conductivity or permittivity of the surface layer.

#### References

- [1] J. P. Gabano, French Patent 7004833 (1970).
- [2] A. N. Dey, *Thin Solid Films* **43** (1977) 131.
- [3] E. Peled, *J. Electrochem. Soc.* **126** (1979) 2047.
- [4] G. L. Holleck and K. D. Brady, in Proc. Symp. on 'Lithium Batteries' (edited by A. N. Dey), The Electrochem. Soc. (1984).
- [5] W. Bowden, J. S. Miller, D. Cubbison and A. N. Dey, *J. Electrochem. Soc.* **131** (1984) 1768.
- [6] A. N. Dey and J. Miller, *J. Electrochem. Soc.* **126** (1979) 1445.
- [7] N. A. Fleischer and R. J. Ekern, *J. Power Sources* **10** (1983) 179.
- [8] D. L. Chua, W. C. Merz and W. S. Bishop, in Proc. of 27th Power Sources Symp., Atlantic City (1976).
- [9] J. P. Gabano and J. Y. Grassien, U.S. Patent 4228229 (1980).
- [10] D. Vallin and P. Chenebault, in Proc. of 32th Power Sources Symp., Cherry Hill (1986).
- [11] T. Kalnoki-Kis, U.S. Patent 4278741 (1981).
- [12] C. R. Schlaikjer, in 'Lithium Batteries' (edited by J. P. Gabano), Academic Press, New York (1983).
- [13] J. W. Boyd, *J. Electrochem. Soc.* **134** (1987) 18.
- [14] M. Drache, Ph.D. Thesis, Lille, France (1979).
- [15] B. Vanderpe and M. Drache, *Bull. Soc. Chim. Fr.* **8** (1971) 2878.
- [16] M. Drache, B. Vanderpe and J. Heubel, *Bull. Soc. Chim. Fr.* **11/12** (1976) 1749.
- [17] M. Garreau and J. Thevenin, *J. Microsc. Spectr. Electron.* **3** (1978) 27.
- [18] P. Chenebault, Ph.D. Thesis, Paris, France (1986).
- [19] M. Bienfait, R. Boistelle and R. Kern, in 'Adsorption et Croissance Cristalline', Colloques Internationaux du C.N.R.S. No. 152, Nancy, France (1965) pp. 515, 577.
- [20] E. Peled, in 'Lithium Batteries' (edited by J. P. Gabano), Academic Press, New York (1983).
- [21] W. I. Archer and R. D. Armstrong, in 'Electrochemistry, Vol. 7' (edited by H. R. Thirsk), Specialist Periodical Reports, The Chemical Society, Burlington House (1978).
- [22] E. J. Schouler, N. Mesbahi and G. Vitter, *Solid State Ionics* **9/10** (1983) 673.

- 
- [23] H. J. de Bruin and A. D. Franklin, *J. Electroanal. Chem.* **118** (1981) 405.
- [24] E. Peled and H. Straze, *J. Electrochem. Soc.* **124** (1977) 1030.
- [25] E. Peled and H. Yamin, in Proc. of 28th Power Sources Symp., Atlantic City (1979).
- [26] R. V. Moshtev, Y. Geronov and B. Puresheva, *J. Electrochem. Soc.* **128** (1981) 1851.
- [27] A. M. Hermann, in Proc. Symp. on 'Lithium Batteries' (edited by V. H. Venkatasety), The Electrochem. Soc. (1981).